Magn Reson Mater Phy (2008) 21:435–442
DOI 10.1007/s10334-008-0156-9

RESEARCH ARTICLE

High resolution magic angle spinning NMR spectroscopy for metabolic assessment of cancer presence and Gleason score in human prostate needle biopsies

Jack J. A. van Asten · Vincent Cuijpers · Christina Hulsbergen-van de Kaa · Claudia Soede-Huijbregts · J. Alfred Witjes · Albert Verhofstad · Arend Heerschap

Received: 8 April 2008 / Revised: 5 November 2008 / Accepted: 5 November 2008 / Published online: 25 November 2008

Abstract
Objectives Histopathology of prostate needle biopsies (PNBs) is an important part in the diagnosis, prognosis and treatment evaluation of prostate cancer. The determination of metabolite levels in the same biopsies may have additional clinical value. Here, we demonstrate the use of non-destructive high resolution magic angle spinning (HRMAS) proton NMR Spectroscopy for the assessment of metabolic profiles of prostate tissue in PNBs as commonly obtained in standard clinical practice.
Materials and methods PNBs that were taken routinely from 48 patients suspected of having prostate cancer were subjected to HRMAS proton NMR spectroscopy. Subsequent histopathology of the same biopsies classified the tissue either as cancer ($n = 10$) or benign ($n = 30$).
Results Some practical aspects of this assessment were evaluated, such as typical spectral contamination caused by the PNB procedure. Significant metabolic differences were found between malignant and benign tissue using a small set of ratio's involving signals of choline compounds, citrate and lactate. Moreover, significant correlations were observed between choline, total choline, and citrate over creatine signal ratios and the Gleason scores of tumor in PNBs and of tumor in the whole prostate.
Conclusion This preliminary study indicates that HRMAS NMR of routinely obtained PNBs can provide detailed metabolic information of intact prostate tissue with clinical relevance.

Keywords Prostate needle biopsy · Prostate cancer · HRMAS NMR Spectroscopy · Gleason score

Albert Verhofstad died before publication of this article.

J. J. A. van Asten (✉) · C. Soede-Huijbregts · A. Heerschap
Department of Radiology, Radboud University
Nijmegen Medical Center, Nijmegen, The Netherlands
e-mail: J.VanAsten@rad.umcn.nl

V. Cuijpers · C. Hulsbergen-van de Kaa · A. Verhofstad
Department of Pathology, Radboud University
Nijmegen Medical Center, Nijmegen, The Netherlands

J. A. Witjes
Department of Urology, Radboud University
Nijmegen Medical Center, Nijmegen, The Netherlands

A. Heerschap (✉)
Department of Radiology (430),
University Medical Center Nijmegen,
P.O. Box 9101, 6500 HB, Nijmegen, The Netherlands
e-mail: A.Heerschap@rad.umcn.nl

Introduction

In spite of the high incidence of prostate cancer (PCa) in western males, the number of patients developing invasive and metastasizing tumors is relatively low. Because advanced disease cannot be cured, early diagnosis is important. Unfortunately, established markers to detect patients with high risk for progressive growth of prostate cancer are still lacking. Hence, there is much interest in the development of an objective, fast and minimal-patient-aggravating diagnostic tool to identify the nature of tumor tissue [1,2]. Histopathological analysis of transrectal ultrasound (TRUS) guided biopsies is commonly used to differentiate between PCa, prostatitis and normal tissue or benign prostatic hyperplasia (BPH) and to characterize tumor grade [3–6]. This analysis may be extended with information on pathological changes in tissue metabolism, which may contribute to a more refined diagnosis or more importantly, a better prognostic evaluation.

In order to acquire information about the metabolic content of prostate tissue, several groups have used high-resolution ^{1}H NMR spectroscopy [7–11]. These studies were performed

on homogenates or on solutions obtained after extraction of prostate tissue material obtained after surgery. To avoid the limitations of tissue homogenization and extraction, prostate tissue samples also can be investigated with high resolution magic angle spinning (HRMAS) NMR [12–14]. By using this technique, originally developed to study combinatorial chemistry products [15], small pieces of intact tissue can be examined with comparable spectral resolution as in solution state NMR. This approach is now commonly applied to tissue obtained by radical prostatectomy.

Here we demonstrate that with HRMAS NMR it is also possible to perform a metabolic analysis of intact prostate tissue obtained by prostate needle biopsy (PNB), to assess the presence and grade of malignancy in the prostate. As these biopsies are taken routinely on out-patient basis in urological practice, the potential clinical impact of the method becomes much broader: not only patients who will receive an operation of the prostate can be included, but also patients with urological diseases who will not be operated [16]. Moreover, as the sample remains intact, histopathology can be performed on the same tissue sample and thus HRMAS NMR with the assessment of metabolism may have a complementary clinical role to standard histopathology.

Materials and methods

Patients and tissues

Patients that clinically were suspected of having prostate cancer were included in this study. All had PSA levels >3 ng/ml. They were subjected to ultrasound guided sextant biopsies to assess the pathological status of prostate tissue. To exclude potential interference with the standard diagnostic procedures from each patient in whom sextant biopsies were taken, one additional prostate needle biopsy (18 GA, ∼5 mg) was taken for HRMAS NMR with the written consent of the patient. The biopsies were immediately snapshot frozen and stored in liquid nitrogen. Based on the histopathology of the sextant biopsies, an expert pathologist divided the cases into two cohorts: malignant ($n = 42$) and benign ($n = 130$). Benign cases with any of the sextant biopsies identified with inflammatory processes, atrophia or atypical hyperplasia, were not further analyzed in this study [4–6]. Based on these criteria, the biopsies of 30 patients (average age 66 years, range 55–80) were included as benign. Malignant PNB cases which did not show PCa in at least two out of three biopsies of either the left or right part of the sextant biopsies, were also excluded from further analysis. Based on this criterion the biopsies of 18 patients (average age at diagnosis 68 years, range 54–80) were included as malignant with adenocarcinoma of the prostate. After the HRMAS NMR investigation, histopathological examination was done on the snapshot-frozen biopsies to classify the nature of the tissue. The pathologist evaluated each snapshot-frozen PNB for presence of PCa and estimated tumor load, which varied from 20 to 95%. The Gleason scores, assessed for tumor tissue in the snapshot-frozen PNBs and in the routine sextant biopsies, ranged from 5 to 10.

HRMAS NMR spectroscopy

HRMAS NMR was performed on a Bruker DRX 500 MHz spectrometer, equipped with a ^{1}H optimized ^{1}H/^{13}C HRMAS probe head. Prior to investigation, the PNB samples were thawed and weighted (2.2–6.9 mg). Tissue material was restricted by Teflon spacers to a 12 µl sphere with a diameter of 2.8 mm placed in a 4-mm ZrO_2 MAS rotor that was sealed with a Kel-F cap. After the PNB has been put into the rotor, the residual space was filled with a 30/70 mixture of PBS-buffer/ D_2O to prevent damage of the tissue. A separate healthy prostate biopsy was measured before and after cutting it to small pieces and adding a 5-µl solution of DNA (500 ng/µl). NMR spectra were acquired at constant room temperature (20°C) [17,33] with a magic angle spinning rate (masr) of 5 kHz, which suppresses the line broadening effects of dipolar coupling and chemical shift anisotropy. The 90° pulse was optimized per sample ranging from 6.2 to 9.5 µs. For 1-D ^{1}H NMR, the CPMG pulse sequence was employed [18]. A T_2 filter of 50 ms was used to suppress contribution of macromolecular components. And an interval of one rotor period (1/masr) between the 180° pulses enabled the suppression of the effects of J-modulation and the minimization of the diffusion component to relaxation processes. The water resonance was suppressed by presaturation. With an excitation bandwidth of 10 ppm collected in 16K points the acquisition time was 1.64 s, and with 256 transients collected every 2 s, the total measurement time was ∼8.5 min. The whole procedure from the start of thawing onward lasted less than 30 min.

After the HRMAS NMR examination the biopsies were snapshot frozen again and used to make cryostat sections for histopathology. The NMR spectra were referenced to the chemical shift value of the creatine methyl resonance at 3.03 ppm [14]. Peak areas were determined by fitting the most important metabolite signals in the frequency domain with optimized combinations of Lorentzian and Gaussian line shapes in Topspin (Bruker Biospin inc.). The metabolite signals analyzed in this way were first normalized per proton: glycero-phosphocholine and phosphoryl choline (GPC + PC at 3.21 ppm/12), choline (Cho at 3.19 ppm/9), polyamines, which are dominated by spermine [11] (Spm at 3.14 ppm/12), creatine (Cr at 3.03 ppm/3) and citrate (Cit at Σ (2.70, 2.67 ppm/2)). Then, the calculated areas of the fitted peaks were normalized to the creatine resonance at 3.03 ppm. The clinically relevant ratios of total choline over citrate (tCho/Cit) and the total choline plus creatine over citrate

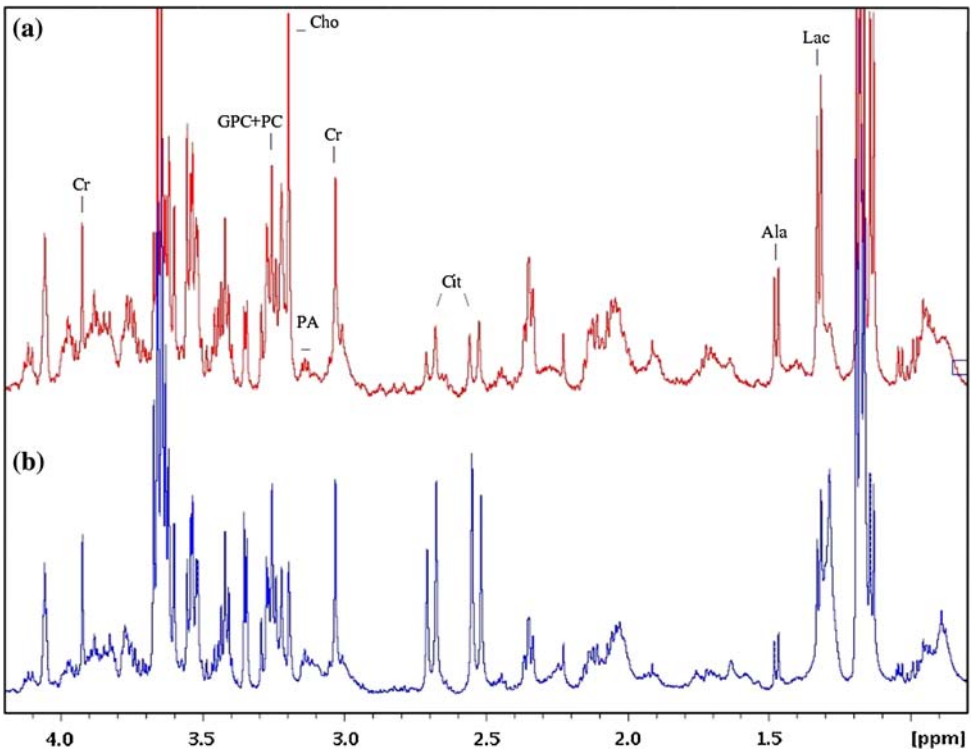

Fig. 1 **a** ^{1}H HRMAS NMR spectrum of a prostate needle biopsy in 30/70 PBS buffer/D2O of tissue material classified as malignant (90 tumor load and Gleason score 7). **b** ^{1}H HRMAS NMR spectrum of a prostate needle biopsy in 30/70 PBS buffer/ D2O of tissue material classified as benign. This spectrum is contaminated with ethanol (triplet at 1.22 ppm and quartet at 3.68 ppm). Annotated resonances are for the metabolites: creatine (*Cr*), glycero-phosphocholine (*GPC*), phosphorylcholine (*PC*), choline (*Cho*), polyamines (*PA*), citrate (*Cit*), alanine (*Ala*) and lactate (*Lac*)

(CC/C) were evaluated. Additionally, the ratio of total choline over citrate and the ratio of the lactate over alanine signals (Lac doublet at 1.33 ppm/Ala doublet at 1.47 ppm) were calculated. Lac/Ala ratios were only evaluated, when a lactate doublet could be identified without lipid contamination. Statistically significant differences between the benign and malignant groups of biopsies were assessed with a two-tailed unpaired t-test, corrected for unequal variances.

Histopathological examination

Four-micrometer-thick frozen sections of the prostate biopsies were mounted on Superfrost Plus slides (Menzel Gläzer, Braunschweig, Germany), fixed in absolute ethanol for 1 min and air-dried. After short rinsing in tap water the slides were stained for 10 min in a hematoxylin solution according to Mayer [19]. Next the slides were counterstained for 5 min with an eosine Y (Merck) staining solution. Finally, the sections were dehydrated quickly in ethanol 95% and absolute ethanol, cleared in xylene and mounted with Permount (Fisher Scientific, Fair Lawn, USA). From each biopsy the pathologist examined at least one section.

Results

HRMAS ^{1}H NMR spectra of high quality could be obtained from prostate needle biopsies showing many resolved resonances of multiple metabolites such as citrate, creatine, polyamines (spermine), lactate and choline (Fig. 1). A detailed metabolic profile of prostate tissue can be obtained relatively fast and basically without destruction of the material. Possible damage of tissue structure due to high spinning rates did not interfere with histopathological diagnosis in our study (Fig. 2).

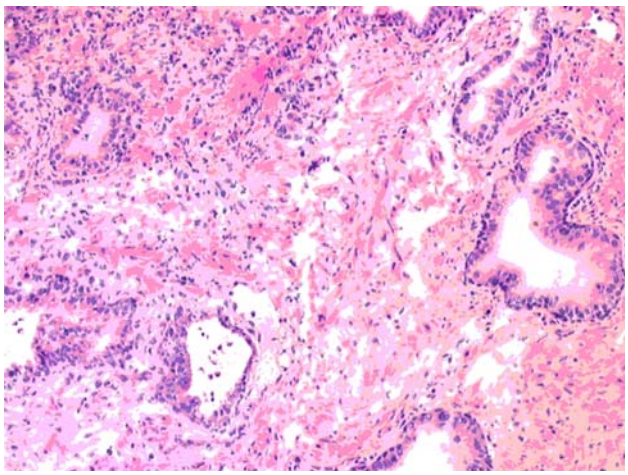

Fig. 2 HE stained frozen tissue section of prostate needle biopsy after approximately 15 min of spinning at 5 kHz

The tissue samples were used directly after defrosting and without washing, preventing a possible wash out of tissue liquid. Proper procedures in the acquisition of PNBs are essential to avoid disturbing contamination of spectra that

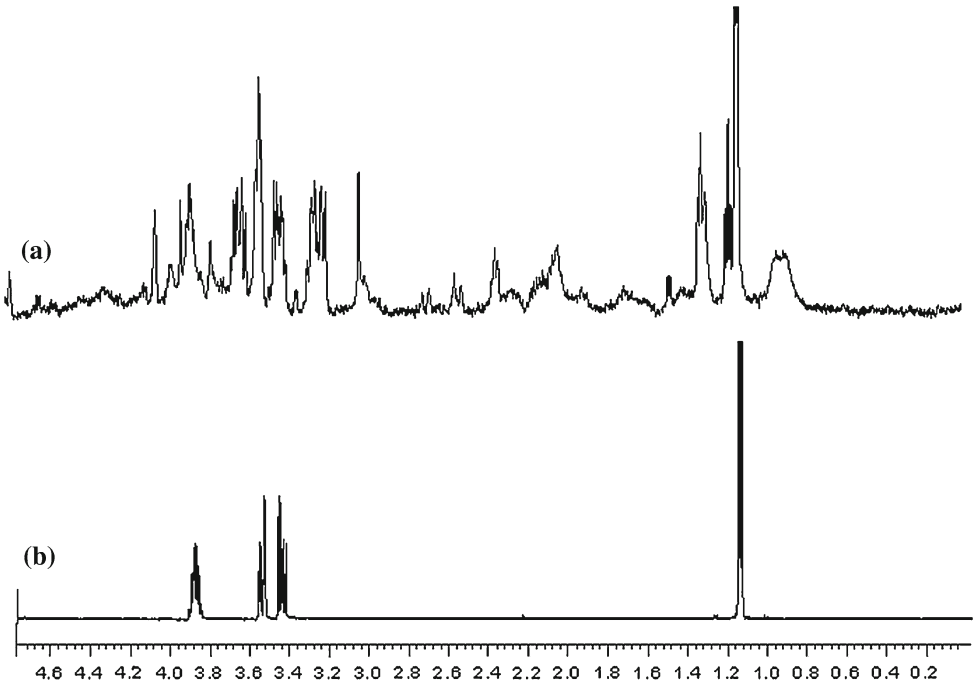

Fig. 3 **a** ^{1}H HRMAS NMR spectrum of prostate needle biopsy contaminated with echo gel signals. **b** ^{1}H HRMAS NMR spectrum of echo gel

will hamper complete analysis of the available metabolic information. For instance, contact of the PNB with echo gel resulted in distorting signals in the HRMAS NMR spectrum (Fig. 3). The presence of these signals can easily be reduced by avoiding contact of the biopsy needle with echo gel used for ultra sound guidance. Further contamination of the spectra sometimes occurred for other reasons. The use of ethanol in handling the tissue, for example, occasionally caused signals of this compound to appear in the spectra (Fig. 1b), and if the PNB includes peri-prostatic fat this may give relatively large lipid signals unless the fat is removed from the biopsy. Polyamine signals are among the most variable in HRMAS spectra of prostate tissue. As the highly positively charged polyamines largely occur in extracellular space they may be prone to interact with negatively charged molecules which may become available upon cell destruction, demonstrated by a decrease of spermine signals (Fig. 4).

From in vivo MR studies it follows that the levels of choline compounds, citrate and polyamines (spermine) may serve as biomarkers in the diagnosis of prostate cancer [26, 28]. Therefore we included relative signal levels of these compounds in the metabolic assessment of malignant and benign biopsies (Table 1). Compared to benign tissue the ratios tCho/Cit, Cho/Cr, (GPC + PC)/Cr and Lac/Ala in PCa are significantly increased in malignant tissue ($p < 0.05$), while the Cit/Cr ratio in PCa is significantly decreased ($p < 0.05$). The (tCho + Cr)/Cit signal ratio (CC/C), which often has been used by in vivo MRS to assess the presence of prostate cancer, is also significantly different ($p < 0.05$) between benign and malignant tissues. The Spm/Cr ratio appeared to be decreased although not significantly. No correlation was found between tumor load and metabolic ratios. Also an analysis of biopsies with more and less than 50% tumor tissue showed only minor differences in accuracy (Table 1). The p values of the ratio differences indicate that a similar discrimination is possible between benign and malignant tissues at higher tumor load.

Finally, the correlation between signal ratios of metabolites and the Gleason score of tumor tissue in the PNBs was assessed. Significant Spearman's rank correlation coefficients were found between the ratios GPC+PC/Cr, Cho/Cr, tCho/Cr, Cit/Cr, tCho/Cit and CC/C ($p < 0.05$) and the Gleason scores. In an evaluation for linear regression a significant correlation was found for the Cho/Cr, tCho/Cr and Cit/Cr ratios with the Gleason score of tumor in the snapshot-frozen PNBs (Fig. 5). Linear regressions for other ratios and Gleason score were not significant, for instance, the CC/C and Lac/Ala ratio only showed weak linear correlations with Gleason score of the PNB's (p values of 0.37 and 0.95, respectively).

Discussion

In this report we describe that prostate needle biopsies can be assessed with HRMAS NMR to obtain metabolic information. The results of this study to detect malignancy in PNB material of patients suspected to have prostate cancer are generally in agreement with those of HRMAS on surgically obtained biopsies [13, 14, 20, 21]. As PNBs are obtained widely in common urological practice this opens the possibility to include metabolic assessment in routine analysis

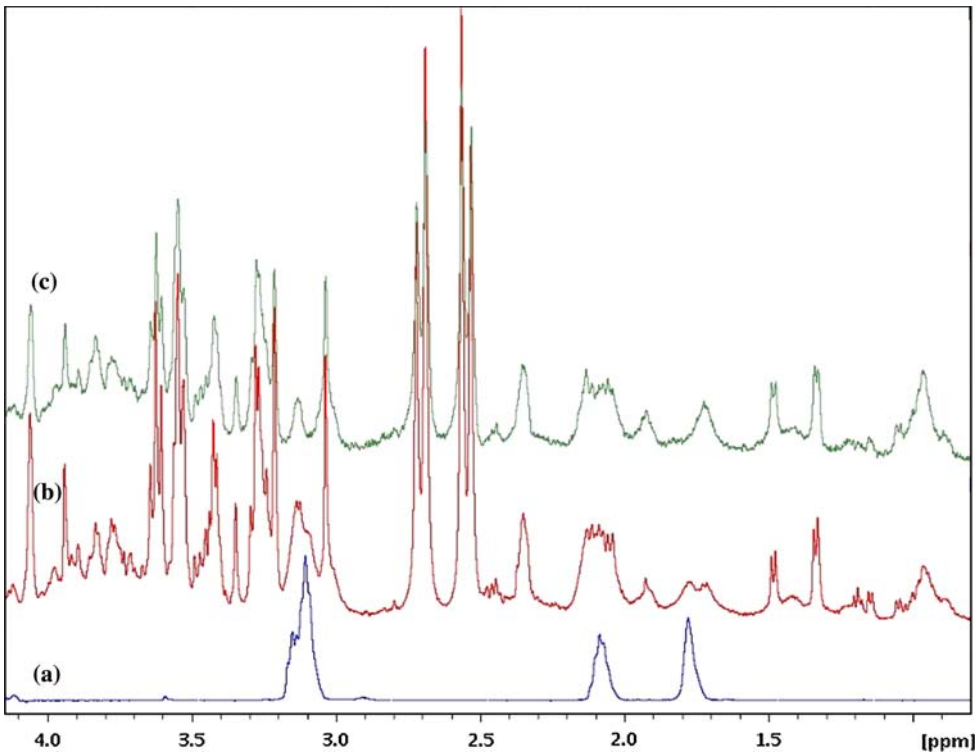

Fig. 4 **a** ^{1}H HRMAS NMR spectrum of spermine. **b** ^{1}H HRMAS NMR spectrum of a fresh prostate needle biopsy of healthy tissue. **c** ^{1}H HRMAS NMR spectrum of the same sample as B after destructing the tissue and mixing with DNA. Besides minor differences due to shimming, the specific signals of spermine are clearly reduced

Table 1 Mean metabolite ratios of prostate needle biopsies of malignant (n = 18) and benign (n = 30) tissue

Tissue	Malignant			Malignant (tumor load > 50%)			Benign	
Metabolite ratio	Ratio	SD	p ($x < 0.05$)	Ratio	SD	p ($x < 0.05$)	Ratio	SD
CC/C	5.52	8.74	0.046	6.68	9.63	0.048	1.03	1.87
tCho/Cit	2.00	3.85	0.021	2.46	4.28	0.009	0.30	0.59
(GPC + PC)/Cr	0.62	0.60	0.046	0.71	0.65	0.035	0.30	0.31
Cho/Cr	0.81	0.45	0.001	0.91	0.41	0.000	0.37	0.22
Spm/Cr	0.05	0.04	0.179	0.05	0.04	0.236	0.09	0.13
Cit/Cr	1.74	1.91	0.010	1.21	0.98	0.000	3.65	2.99
Lac/Ala	8.35	7.35	0.032	8.41	7.85	0.048	3.05	1.92

SD Standard deviation. *CC/C* is the total choline plus creatine over citrate ratio. For the Lac/Ala ratio of the malignant biopsies, $n = 9$ and for those with tumor load >50%, $n = 8$ and for the benign biopsies, $n = 21$. Reported p values are given for malignant tissue with respect to benign tissue

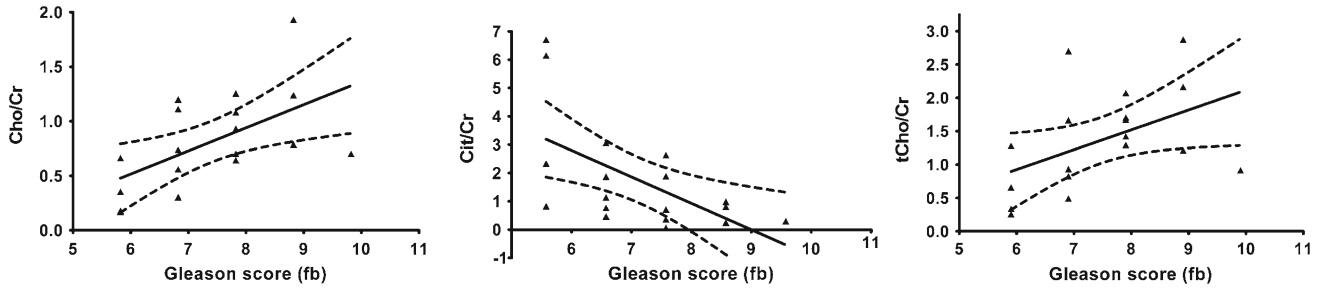

Fig. 5 Linear regression plots of Cho/Cr (*left*) and Cit/Cr (*middle*) and tCho/Cr (*right*) metabolic ratios to Gleason score of snapshot frozen prostate needle biopsies ($n = 18$) with p values of, respectively, 0.014, 0.011, 0.049

of biopsies, which may help to refine diagnosis and might have additional prognostic value. This approach is particularly attractive as it allows for further histopathological examinations after the HRMAS measurement, albeit within the limits of frozen section morphology.

Some practical aspects of HRMAS NMR measurements of prostate tissue have been addressed previously [21,22]. In this study we show that the biopsy procedure to obtain PNBs may result in HRMAS NMR spectra with signals from specific contaminations, interfering with spectral analysis, which, however, largely can be avoided if proper precautions are taken into account. Polyamine signals are rather variable in prostate biopsy spectra [21], which may depend on the preparation method. For instance, spermine may be affected by electrostatic binding to other molecules or by enzymatic breakdown during the biopsy harvesting and measurement procedure.

There is some concern that the rapid spinning of the sample may cause tissue alterations interfering with proper histopathological analysis [23]. However, in our experiments with small diameter samples this problem did not arise, but obviously the implementation of slow spinning methods is advisable to avoid any possible ambiguity on this matter in the future. Alternative methods of this kind have been reported [23,24].

To target biopsy sampling from specifically diseased prostate tissue is not trivial, as diseases like prostate cancer are known to be very heterogeneous and multi-focal, and nodules are hard to find with TRUS. Cancer and chronic inflamed tissue are not easily found with TRUS because they are often not visible as a hypo-echogenic area. Therefore, we classified the patient specimens only on the basis of the histopathological findings in the PNBs that were measured by HRMAS NMR. For a first analysis we selected a limited number of resonances, i.e., of creatine, choline compounds (choline, glycero-phosphocholine, phosphorylcholine), polyamines (predominantly spermine), lactate, alanine and citrate because the signals of these metabolites play a (potential) role as biomarkers in the assessment of prostate cancer by in vivo MR Spectroscopy [25–29]. Although the variance among metabolite levels determined from HRMAS NMR spectra is high, significant discrimination between the malignant and benign tissues could be achieved by the analysis of a small set of different metabolite signal ratios. Among these are the signals of citrate, a compound whose level is known to be reduced in prostate tumor tissue [25–28]. Citrate is produced in epithelial tissue and excreted in the lumen of the prostate, where it appears to go together with polyamines [30]. Changes in citrate tissue levels may be caused by altered metabolism [31], but suppression of the luminal space because of tumor growth is likely an important factor in this decrease. Polyamines are a group of compounds of particular interest [11], for which also a decreased signal intensity could be expected in tumor tissue because of its ductal origin. The relative Spm signals indeed are decreased, but not significantly, the reason for which is discussed earlier. The levels of choline compounds are known to be elevated in tumor tissue, which has been assigned to increased cell proliferation, associated with altered choline metabolism in tumors [8,25–27,29].

Tissue levels of lactate and alanine may increase due to hypoxia, which may have occurred during the biopsy procedure even though the samples were rapidly frozen. In a previous HRMAS NMR study on prostate tissue very little changes in lactate and alanine levels were observed over time, which probably was due to the depletion of glucose [22]. Although the total level of lactate and alanine may differ per sample, the ratio of these two appears to be a biomarker for prostate cancer. In tumors specific lactate increase is associated with aerobic glycolysis [32]. The significantly increased lactate over alanine ratio observed for malignant tissue may be of interest in the visualization of prostate cancer by metabolic imaging with hyperpolarized ^{13}C MR [33].

The tumor load per biopsy sample may affect typical tumor metabolite ratios and therefore hamper proper interpretation of the data. But, no significant correlation between tumor load and metabolite ratios was found. Specific statistical approaches may be able to separate metabolite profiles of subcomponents in heterogeneous prostate tissues [34].

From a clinical point of view, the significant linear regressions found for Cho and Cit ratio's with the Gleason scores of the tumor snapshot frozen PNBs are more interesting. This has not been reported previously for surgical prostate material, but correlations have been observed for metabolite ratios obtained from in vivo MR spectra and Gleason score [35,36]. Several studies have observed that abnormal choline metabolism is associated with the malignancy of cancer cells, e.g., [37,38]. No significant linear regression was found for the CC/C ratio with Gleason score which indicates that separate observation of choline and creatine peaks is desirable in grading of prostate cancer by MR spectroscopy. At least part of the variation seen for metabolite ratios in the malignant samples (Table 1) can be attributed to variable Gleason scores. Some variation in the ratios of benign tissue may be due to different contributions of glandular and stromal tissue [21].

Analyzing the data of the HRMAS NMR measurements of PNBs with a multi-variate approach [39], is expected to strongly improve the clinical significance in diagnosis and prognosis. A more comprehensive spectral analysis also could be helpful in this respect. As the sample remains intact, histopathology can be performed on the same tissue sample and thus complementary metabolomics and histopathological assessment of these samples is possible. Full assessment of the potential of this functionality requires studies of a larger number of PNB samples including those with

other prostate diseases such as prostatitis. In these studies it will be relevant to correlate the data with specific histopathological findings, apart from Gleason score, or other findings, such as PSA and genomic and proteomic data.

Acknowledgments We thank Mrs. Gerda Nachtegaal for valuable technical assistance. This research was supported by a grant of the Dutch Cancer Society (KUN 98-1812).

References

1. Thornbury JR, Ornstein DK, Choyke PL, Langlotz CP, Weinreb JC (2001) Prostate cancer: what is the future role for imaging. AJR Am J Roentgenol 176:17–22
2. Gao X, Porter AT, Grignon DJ, Pontes JE, Honn KV (1997) Diagnostic and prognostic markers for human prostate cancer. Prostate 31:264–281
3. Deshmukh N, Foster CS (2002) Grading prostate cancer. In: Foster CS, Bostwick DG (eds) Pathology of the prostate. W.B. Saunders Company, Philadelphia, pp 191–227
4. Matsumoto T, Mochida O, Kumazawa J, Kinjo M, Sagiyama K (2002) Critical assessment of inflammatory lesions of the prostate, including cytopathologic appearances and diagnosis. In: Foster CS, Bostwick DG (eds) Pathology of the prostate. W.B. Saunders Company, Philadelphia, pp 56–65
5. Nickel JC, True LD, Krieger JN, Berger RE, Boag AH, Young ID (2001) Consensus development of a histopathological classification system for chronic prostatic inflammation. BJU Int 87:797–805
6. Helpap B (2002) Benign prostatic hyperplasia. In: Foster CS, Bostwick DG (eds) Pathology of the Prostate. W.B. Saunders Company, Philadelphia, pp 66–113
7. Schiebler ML, Miyamoto KK, White M, Maygarden SJ, Mohler JL (1993) In vitro high resolution ^{1}H-spectroscopy of the human prostate: benign prostaic hyperplasia, normal peripheral zone and adenocarcinoma. Magn Reson Med 29:285–291
8. Cornel EB, Smits GA, Oosterhof GO, Karthaus HF, Schalken JA, Heerschap A (1993) Characterization of human prostate cancer, benign prostatic hyperplasia and normal prostate by in vitro ^{1}H and ^{31}P magnetic resonance spectroscopy. J Urol 150: 2019–2024
9. Kurhanewicz J, Dahiya R, MacDonald JM, Chang LH, James TL, Narayan P (1993) Citrate alterations in primary and metastatic human prostatic adenocarcinomas: ^{1}H magnetic resonance spectroscopy and biochemical study. Magn Reson Med 29:149–157
10. Hahn P, Smith IC, Leboldus L, Littman C, Somorjai RL, Bezabeh T (1997) The classification of benign and malignant human prostate tissue by multivariate analysis of ^{1}H magnetic resonance spectra. Cancer Res 57:3398–3401
11. van der Graaf M, Schipper R, Oosterhof G, Schalken J, Verhofstad A, Heerschap A (2000) Proton MR spectroscopy of prostatic tissue focused on the detection of spermine, a possible biomarker of malignant behavior in prostate cancer. MAGMA 10:153–159
12. Tomlins AM, Foxall PJD, Lindon JC, Lynch MJ, Spraul M, Everett JR, Nicholson JK (1998) High resolution magic angle spinning H-1 nuclear magnetic resonance analysis of intact prostatic hyperplastic and tumour tissues. Anal Commun 35:113–115
13. Cheng LL, Wu C, Smith MR, Gonzalez RG (2001) Non-destructive quantitation of spermine in human prostate tissue samples using HRMAS ^{1}H NMR spectroscopy at 9.4 T. FEBS Lett 494:112–116
14. Swanson MG, Vigneron DB, James JK, Kurhanewicz J (2002) ^{1}H HR-MAS investigations of four potential markers for prostate cancer. Proc Int Soc Mag Reson 9:2336
15. Fitch WL, Detre G, Holmes CP (1994) High resolution ^{1}H NMR in solid-phase organic synthesis. J Org Chem 59:7955–7956
16. Smith ICP, Blandford DE (1998) Diagnosis of cancer in humans by ^{1}H NMR of tissue biopsies. Biochem Cell Biol 76:472–476
17. Huhn Stephen D, Szabo Christina M, Gass Jerome H, Manzi Adriana E (2004) Metabolic profiling of normal and hypertensive rat kidney tissues by hrMAS-NMR spectroscopy. Anal Bioanal Chem 378:1511–1519
18. Meiboom S, Gill D (1958) Modified Spin-echo Method for measuring nuclear relaxation times. Rev Sci Instrum 29:688–691
19. Bancroft JD, Stevens A, Turner DR (1996) Theory and practice of histopathological techniques. Churchill Livingstone, New York, p 101
20. Swanson GM, Vigneron DB, Tabatabai ZL, Males RG, Schmitt L, Carroll PR, James JK, Hurd RE, Kurhanewicz J (2003) Proton HR-MAS spectroscopy and quantitative pathologic analysis of MRI/3D-MRSI-targeted postsurgical prostate tissues. Magn Reson Med 50:944–954
21. Swanson MG, Zektzer AS, Tabatabai ZL, Simko J, Jarso S, Keshari KR, Schmitt L, Carroll PR, Shinohara K, Vigneron DB, Kurhanewicz J (2006) Quantitative analysis of prostate metabolites using ^{1}H HR-MAS spectroscopy. Magn Reson Med 55:1257–1264
22. Wu CL, Taylor JL, He W, Zepeda AG, Halpern EF, Bielecki A, Gonzalez RG, Cheng LL (2003) Proton high-resolution magic angle spinning NMR analysis of fresh and previously frozen tissue of human prostate. Magn Reson Med 50:1307–1311
23. Wind RA, Hu JZ, Rommereim DN (2001) High-resolution ^{1}H NMR spectroscopy in organs and tissues using slow Magic Angle Spinning. Magn Reson Med 46:213–218
24. Taylor JL, Wu CL, Cory D, Gonzalez RG, Bielecki A, Cheng LL (2003) High-Resolution Magic Angle Spinning Proton NMR Analysis of Human Prostate Tissue With Slow Spinning Rates. Magn Reson Med 50:627–632
25. Kurhanewicz J, Vigneron DB, Nelson SJ, Hricak H, MacDonald JM, Konety B, Narayan P (1995) Citrate as an in vivo marker to discriminate prostate cancer from benign prostatic hyperplasia and normal prostate peripheral zone: detection via localized proton spectroscopy. Urology 45:459–466
26. Heerschap A, Jager GJ, van der Graaf M, Barentsz JO, de la Rosette JJMCH, Oosterhof GON, Ruijter ETG, Ruijs SHJ (1997) In vivo proton MR spectroscopy reveals altered metabolite content in malignant prostate tissue. Anticancer Res 17:1455–1460
27. Kurhanewicz J, Vigneron DB, Males RG, Swanson MG, Yu KK, Hricak H (2000) The prostate: MR imaging and spectroscopy. Present and future. Radiol Clin North Am 38:115–138
28. Shah N, Sattar A, Benanti M, Hollander S, Cheuck L (2006) Magnetic resonance spectroscopy as an imaging tool for cancer: a review of the literature. J Am Osteopath Assoc 106(1): 23–7
29. Futterer JJ, Scheenen TW, Heijmink SW, Huisman HJ, Hulsbergen-Vande Kaa CA, Witjes JA, Heerschap A, Barentsz JO (2007) Standardized threshold approach using three-dimensional proton magnetic resonance spectroscopic imaging in prostate cancer localization of the entire prostate. Invest Radiol 42(2):116–122
30. Lynch MJ, Nicholson JK (1997) Proton MRS of human prostatic fluid: correlations between citrate, spermine, and myo-inositol levels and changes with disease. Prostate 30:248–255
31. Costello LC, Franklin RB (2006) The clinical relevance of the metabolism of prostate cancer; zinc and tumor suppression: connecting the dots. Mol Cancer 5:17
32. Kim J-w, Dang CV (2006) Cancer's molecular sweet tooth and the Warburg effect. Cancer Res 66:8927–8930

33. Golman K, In 't Zandt R, Thaning M (2006) Real-time metabolic imaging. Proc Natl Acad Sci USA 103(30):11270–11275
34. Stoyanova R, Swanson MG, Vigneron DB, Kurhanewicz J, Brown TR (2002) Metabolite Profiles Associated with Prostate Tissue Subcomponents, Proc Intl Soc Mag Reson Med, 10
35. Zakian KL et al (2005) Correlation of proton MR spectroscopic imaging with gleason score based on step-section pathologic analysis after radical prostatectomy. Radiology 234(3):804–814
36. Kurhanewicz J, Swanson MG, Nelson SJ, Vigneron DB (2002) Combined magnetic resonance imaging and spectroscopic imaging approach to molecular imaging of prostate cancer. J Magn Reson Imaging 16(4):451–463. Review
37. Podo F (1999) Tumour phospholipid metabolism. NMR Biomed 12(7):413–439. Review
38. Glunde K, Jacobs MA, Bhujwalla ZM (2006) Choline metabolism in cancer: implications for diagnosis and therapy. Expert Rev Mol Diagn 6(6):821–829
39. Cheng LL, Burns MA, Taylor JL, He W, Halpern EF, McDougal WS, Wu CL (2005) Metabolic Characterization of Human Prostate Cancer with Tissue Magnetic Resonance Spectroscopy. Cancer Res 65:3030–3035